Lühr, H., Kervalishvili, G., Rauberg, J., Stolle, C. (2016): Zonal currents in the F-region deduced from Swarm constellation measurements. - *Journal of Geophysical Research*, *121*, 1, pp. 638–648.

DOI: http://doi.org/10.1002/2015JA022051

AGU PUBLICATIONS

JGR

Journal of Geophysical Research: Space Physics

RESEARCH ARTICLE
10.1002/2015JA022051

Key Points:
- The Swarm satellite constellation is used for determining current density
- We provide the latitudinal and local time distribution of zonal currents in the topside ionosphere
- F region zonal currents are directed eastward on the dayside and westward on the night side

Correspondence to:
H. Lühr,
hluehr@gfz-potsdam.de

Citation:
Lühr, H., G. Kervalishvili, J. Rauberg, and C. Stolle (2016), Zonal currents in the *F* region deduced from Swarm constellation measurements, *J. Geophys. Res. Space Physics*, *121*, 638–648, doi:10.1002/2015JA022051.

Received 19 OCT 2015
Accepted 10 DEC 2015
Accepted article online 15 DEC 2015
Published online 16 JAN 2016

Zonal currents in the *F* region deduced from Swarm constellation measurements

Hermann Lühr[1], Guram Kervalishvili[1,2], Jan Rauberg[1], and Claudia Stolle[1]

[1]GFZ, German Research Centre for Geosciences, Potsdam, Germany, [2]Iv. Javakhishvili Tbilisi State University, M. Nodia Institute of Geophysics, Tbilisi, Georgia

Abstract The Swarm constellation has been used to estimate zonal currents in the topside *F* region ionosphere at about 500 km. Near-simultaneous magnetic field measurements from two altitudes but the same meridian are used for the current density calculations. We consider the period 15 February to 23 June 2014 for deriving a full 24 h local time coverage of the latitudinal distribution over ±50° in magnetic latitude. Intervals with close orbital phasing at the two heights are considered, which repeat every 6 days. From such days seven successive orbits are used where the epochs of equator crossings differ by less than 2 min. Deduced current densities are predominantly eastward (about 20 nA/m^2) on the dayside and westward (about 10 nA/m^2) on the nightside. A number of different drivers contribute to the observed total current. We identified the gravity-driven eastward current as the most prominent at low latitudes. Eastward currents in the Northern Hemisphere are clearly stronger than in the south. This is attributed to the proximity of our study period to June solstice, when the solar radiation is stronger in the north. In addition, interhemispheric winds from the Northern (summer) to the Southern (winter) Hemisphere contribute. They cause eastward currents in the north and westward in the south. We find a relatively large variability of the zonal currents both in space and time. The standard deviation is at least twice as large as the mean value of current density. This large variability is suggested to be related to gravity wave forcing from below.

1. Introduction

The ionosphere is characterized by a collision-dominated plasma comprising a mixture of charged and neutral particles. The presence of the geomagnetic field causes a highly anisotropic conductivity distribution. Along the field lines currents can flow almost unimpeded. Conversely, transverse conductivities vary significantly with altitude. For example, Hall currents, flowing perpendicular to the electric and magnetic fields, dominate around 110 km altitude. Above 120 km the Pedersen conductivity, supporting currents aligned with the *E* field, is larger. At even higher altitudes, in the ionospheric *F* region, also other forces besides the *E* field become important for driving currents. Well-known mechanisms are the wind-driven *F* region dynamo [*Rishbeth*, 1971; *Lühr and Maus*, 2006], the electron density gradient currents [*Kelley*, 2009; *Lühr et al.*, 2003], or the gravity-driven currents [*Eccles*, 2004; *Maus and Lühr*, 2006]. In sum, all these *F* region currents at middle and low latitudes are expected to be weak, some tens of nA/m^2. Field-aligned currents at middle and low latitudes have recently been deduced reliably from magnetic field measurements of the Swarm satellite constellation [*Lühr et al.*, 2015]. They are mainly driven by potential differences in the two hemispheres related to the Sq current systems.

Horizontal *F* region currents have so far not been studied in details because of the difficulties to measure them. In ground-based magnetic recordings their effect is not visible, and in single-satellite measurements they are commonly masked by the larger signal from field-aligned currents. By applying vector potential analysis to Magsat magnetic field data, *Olsen* [1997] provided global estimates of the radial current component for the morning and evening time sectors. The results confirmed a number of earlier predicted current systems like the radial current above the dip equator in the evening and the interhemispheric field-aligned currents. The limitation of the data set to morning and evening time zones did not allow for general conclusions. First attempts of deducing zonal currents in the *F* region from *B* field measurements at two altitudes were conducted by *Shore et al.* [2013] by considering CHAMP and Ørsted data whenever the spacecraft were crossing over. Periods of near-simultaneous crossovers occurred 24 times during the years 2000 through 2005. Deduced zonal current densities scattered a lot both in amplitude and direction but stayed generally below 20 nA/m^2. The authors could not present a clear local time pattern of current density due to the sparse distribution of conjunction events.

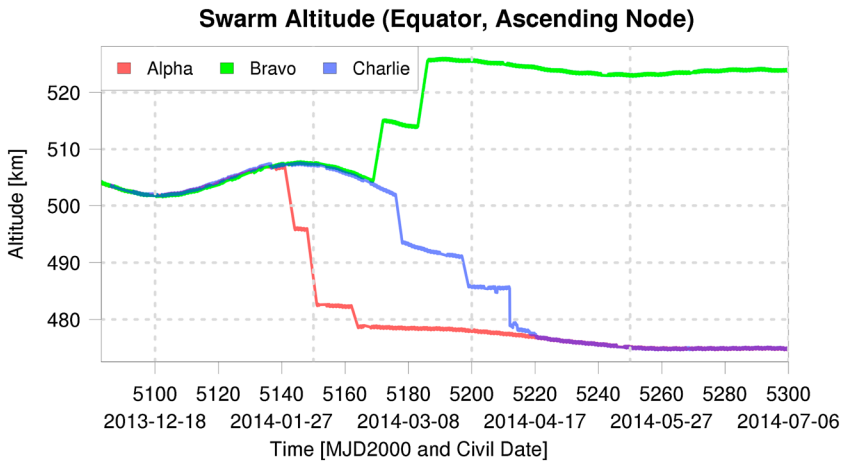

Figure 1. Evolution of orbital altitudes for the three Swarm spacecraft during the early mission period. The altitude is calculated with respect to an Earth radius of 6371.2 km.

With the advent of ESA's constellation mission Swarm we have the possibility to make a new attempt to better resolve the *F* region zonal current distribution. The identical instrumentation on all three spacecraft and the dedicated orbit constellation make the obtained results more reliable. During the commissioning phase the spacecraft Swarm B is maneuvered up to 520 km altitude and Swarm A/C down to 470 km. In a recent study *Tozzi et al.* [2015] applied a statistical analysis to geographically binned magnetic field data from the Swarm constellation. By employing the curl-B relation to the spatially distributed bin averages at two altitudes, they derive average values of the three current components in the topside *F* region. The analysis is limited to quiet time nights within the interval 15 March to 28 September 2014. They estimated average current distributions for two local time sectors, one before and another after midnight. Mean zonal currents obtained at middle and low latitudes are 10–20 nA/m^2 westward at nighttime.

Remaining questions are the local time variation of *F* region currents and an assessment of the prime drivers for the zonal currents. We are trying to resolve these issues. Data from periods are considered when the orbital phasing between Swarm A and B at two altitudes were closely matching. In this study we provide for the first time full local time coverage of the average zonal current density at middle and low latitudes.

In the sections to follow we will first introduce the data and processing approaches. In section 3 two examples of zonal current estimates are presented, and details are discussed. Section 4 contains a statistical analysis of the local time distribution. Since the zonal currents in the topside *F* region are small, section 5 is dedicated to an assessment of involved variability and uncertainties. In the discussion, section 6, we compare our results with previous findings and evaluate the contributions of different drivers to the total zonal current. Finally, we provide a summary and draw conclusions derived from our observations.

2. Data and Processing

2.1. Mission and Data

The Swarm constellation mission [*Friis-Christensen et al.*, 2008] was launched on 22 November 2013 into a near-polar, circular orbit at 490 km altitude. After separation from the rocket all three satellites were flying in close formation during the first 3 months. Altitude maneuveres started in the beginning of February 2014. The actual altitude evolution of the three spacecraft is depicted in Figure 1. First Swarm A is lowered to 470 km, then Swarm B is raised to 520 km. Finally, Swarm C is brought down to the same altitude as Swarm A. First current density estimates could be obtained on 15 February 2014. All orbits with near-simultaneous equator crossings, up to 23 June 2014, were considered for current estimates. This time span is required by the Swarm mission to cover all local times once. During these 130 days the longitudinal separation between Swarm A and B orbits increased continuously from 0.5° to 7.8° at the equator.

Current density estimates are based on readings of the Vector Field Magnetometer. Data of the vector instrument are routinely calibrated, as part of ESA's standard processing, against the Absolute Scalar Magnetometer. For our

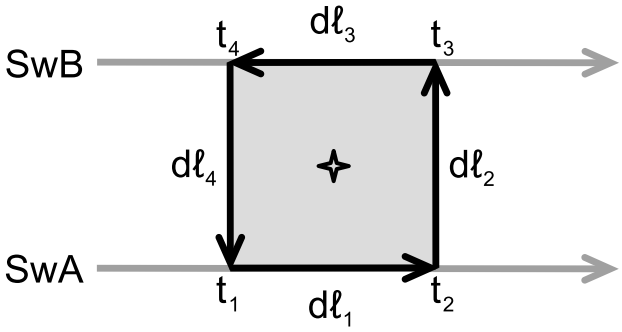

Figure 2. Sketch of the quad of four measurement points needed for the calculation of mean zonal current density at the center. Points 1 through 4 are positions on the orbit tracks of satellites Swarm A and Swarm B connected by route elements *dl*. Measurement points on the Swarm B orbit are on the same magnetic latitudes as Swarm A but sampled at slightly different times.

analysis we used the Level 1b MAGx version 03xx data. Subsequently, we corrected them for the thermomagnetic disturbance. These processing steps ensure high accuracy of the independent magnetic field data sets from the three spacecraft.

In addition to the magnetic field, we also consider the local electron density in this study. It is derived from the Langmuir Probe readings on board the spacecraft.

2.2. Data Processing Approach

For estimating the zonal current density, *j*, we make use of Ampère's integral law:

$$j = \frac{1}{\mu_0 A} \oint \boldsymbol{B}\mathrm{d}\boldsymbol{l} \qquad (1)$$

where *A* is the area encircled by the contour, ***B*** the magnetic field caused by the current, ***dl*** the line element along the integration path, and μ_0 the permeability of free space. In principle the same approach is applied as developed by *Ritter et al.* [2013] for radial currents. However, here we consider a loop in the meridional plane. Swarm A is taken as reference satellite. As shown in Figure 2, two readings are taken along the track, separated by 5 s. When considering the orbital velocity of 7.6 km/s, this corresponds to a distance of 38 km. The radial separation between the satellites A and B amounts to about 50 km. The two corresponding measurements from Swarm B are taken at the same magnetic latitudes as those of Swarm A. The magnetic coordinate system used here is based on the definition by *Richmond* [1995]. From the readings at the four corners of the quad the average zonal current density, j_y, within the encircled area is calculated in a discrete form:

$$j_y = \frac{1}{2\mu_0 A}\left[(Bx_{t1} + Bx_{t2})\, dl_1 + (Bz_{t2} + Bz_{t3})dl_2 - (Bx_{t3} + Bx_{t4})dl_3 - (Bz_{t4} + Bz_{t1})\, dl_4\right] \qquad (2)$$

where *Bx* and *Bz* are the field components at the four corners aligned with the tracks and the vertical directions, respectively; *dl* are the line elements (dl_1, dl_3 along track and dl_2, dl_4 height differences) (see Figure 2). The encircled area is $A = ¼\ (dl_1 + dl_3)(dl_2 + dl_4)$. In order to isolate the magnetic effect caused by the ionospheric currents, the core field, crustal field, and large-scale magnetospheric field have to be removed. This is achieved by subtracting the recent field model CHAOS-5 [*Finlay et al.*, 2015] from the original readings. It should be noted here that a ring integral is used for calculating the current density. Since integrating a potential field along a closed loop gives zero, small deficits of the CHAOS model should not influence the results. Furthermore, the field residuals are low pass filtered with a 3-dB cutoff period of 20 s to avoid the effect of spatial aliasing. We calculate current densities only for orbits where the equator crossing times differ between Swarm A and B by less than 2 min.

3. Characteristics of Zonal *F* Region Currents

Before showing the average distribution of zonal currents, we want to discuss some details of the estimates by looking at examples. There is one interval of close orbital phasing of all three satellites. On 15 February 2014 Swarm A has already been lowered, but Swarm B and C are still in their injection orbits (see Figure 1). For that day we have independent current estimates from the pairs Swarm A/B and Swarm A/C. First, we may have a look at the magnetic field data that are used in the four terms of equation (2). Figure 3 shows latitudinal profiles of these components, in the top row from the pair Swarm A/B and the bottom row from Swarm A/C. It is convincing to see how similar the magnetic field profiles are from the three satellites (curves from Swarm A (blue lines) are repeated in the two rows), both for the horizontal (*Bx*) and vertical (*Bz*) components. This implies that zonal currents at 490 km are weak but also that there are no significant biases between the readings of the different satellites.

From all passes with good Swarm conjunctions we calculated current density according to equation (2). Figure 4 presents two examples from the 1900 magnetic local time (MLT) sector. The top frame reflects results from the data shown in Figure 3. Time and position of the barycentre are given in the header and subframes.

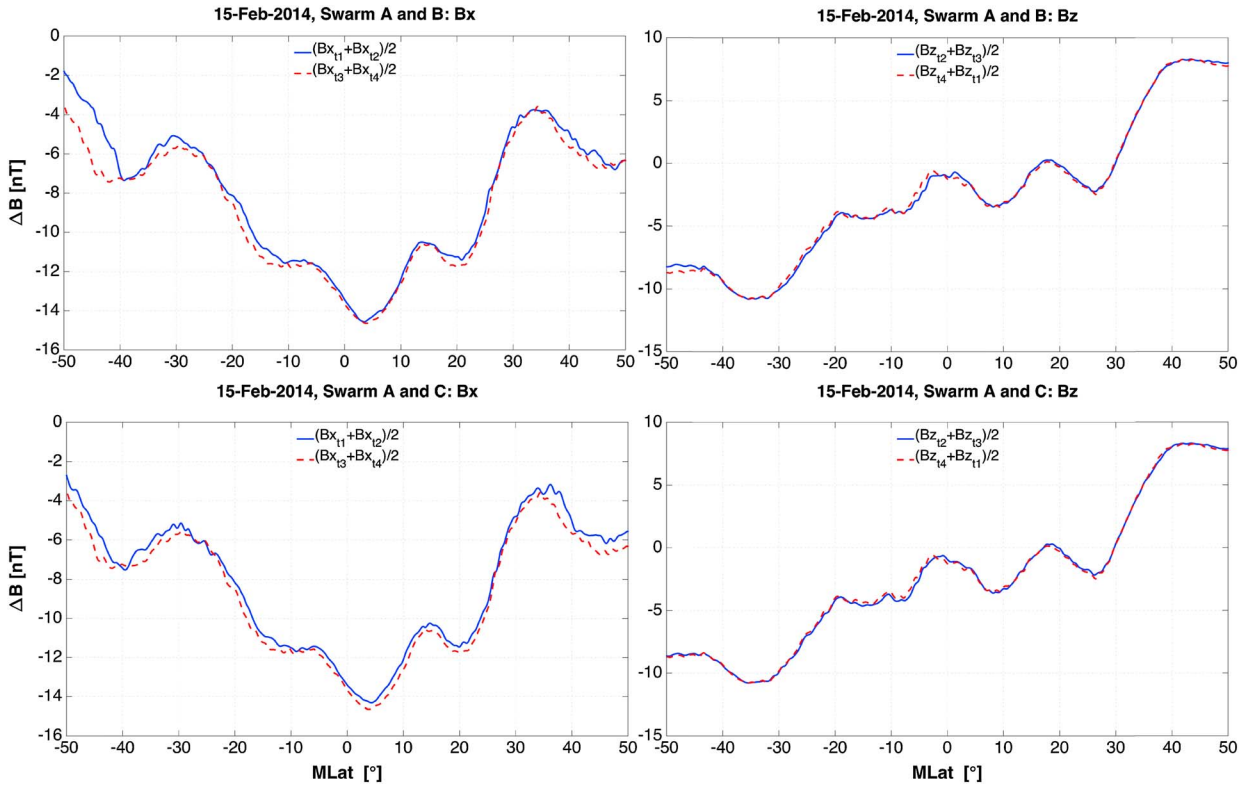

Figure 3. Magnetic field residuals of the components aligned with the four branches of the integration quad. The top row is from the pair Swarm A/B and the bottom row from Swarm A/C. The independently measured magnetic fields from all three satellites agree well. Data are from an orbit that crossed the equator around 07:30 UT.

Results from the two pairs are plotted in different color (Swarm A/B in blue and Swarm A/C in red). At this topside *F* region altitude (491 km) the current densities is fairly low, generally below 30 nA/m^2. The mean level of current strength obtained from the two pairs agrees quite well. But in detail, the latitudinal profiles are different although the measurement times differ only by about 2 min, and the longitude agrees within 0.3°. In case of the second example (Figure 4, bottom frame) the differences are larger. The zonal currents obviously vary a lot both in time and space. The amplitude of variability is typically exceeding the level of mean current density by at least an order of 2. Variations are observed over a wide range of wavelengths in latitudinal direction. This characteristic of current dynamics has to be kept in mind when interpreting the average distribution. In section 5 we will present an assessment of the uncertainties expected for our current density estimates.

4. Local Time Variation of Zonal Current Distribution

As mentioned before, Swarm measurements of 130 days have to be considered for obtaining a full 24 h local time coverage. Alignments of orbital phasing between Swarm A and B occurred every 6 days. From those days seven successive orbits (out of 15 per day), satisfying the 2 min time difference limit, can be used for calculating zonal current densities. As a consequence, we cannot provide a continuous coverage in time but have to use a statistical interpretation. Nevertheless, this is the best that can be made out of the Swarm constellation measurements in terms of local zonal *F* region current estimates with our approach, and it has not been provided by any previous mission. When checking the magnetic activity of the days considered, we found $Ap = 17$ on one day. Only on two more days the value $Ap = 10$ is exceeded. For that reason our results represent quiet time conditions.

Figure 5 shows for middle and low latitudes the zonal current density distribution in a magnetic latitude (MLAT) versus magnetic local time (MLT) frame. Data have been sorted into bins of 1 h in MLT and 5° in MLAT. Presented are bin averages. The number of 1 s readings in each bin varies between 400 and 1400. White areas in the figure represent regions with very low current density. On the nightside we find

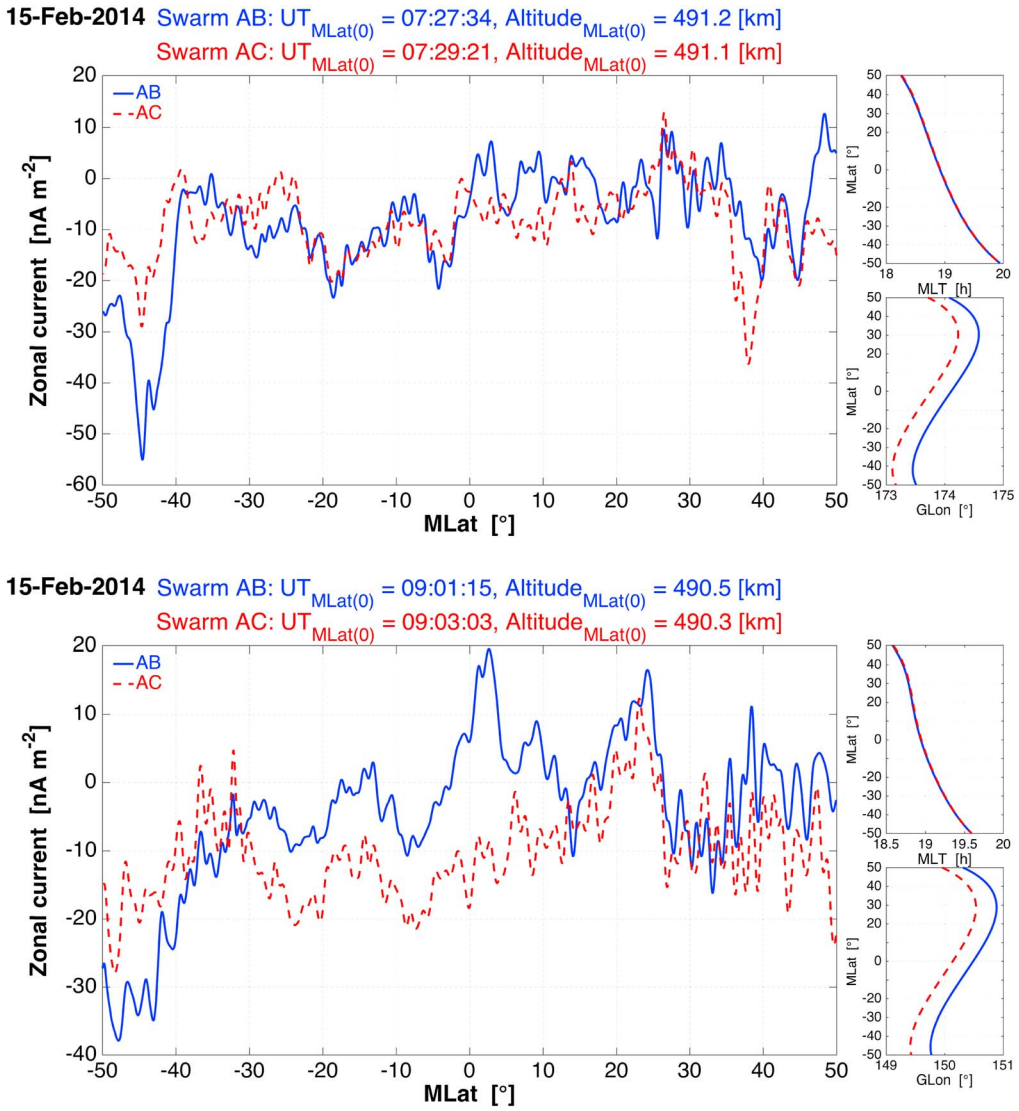

Figure 4. Latitudinal profiles of *F* region zonal currents derived from the pairs Swarm A/B (blue) and Swarm A/C (red). Some significant differences appear between the profiles, although they are separated only a little in time and space. The current profiles shown in the top panel are derived from the magnetic fields presented in the previous figure. The subframes to the right show the magnetic local time (MLT) and the longitude along the orbit.

systematically weak westward currents ranging between 0 and 20 nA/m^2. On the dayside a more complicated distribution emerges. Generally, current densities are stronger in the Northern Hemisphere. This may be due to the prevailing summer conditions. For most of the MLT hours eastward currents in the range 10 to 30 nA/m^2 are observed. The more intense westward currents around 0800 MLT seem to be a spurious effect and is therefore covered by a hashed bar. Possible reasons will be discussed later. In the Southern Hemisphere we find predominantly weak eastward currents in the 0700 to 1300 MLT sector and westward currents thereafter. In both hemispheres eastward currents tend to peak at the equatorial ionization anomaly crests about 10° in latitude away from the magnetic equator. Quite interesting is a tong of westward current close to the dip equator shortly after noon.

The interpretation of the deduced *F* region zonal currents is not so straightforward because of the interleaving seasonal and local time variations. At the beginning of the data period, 15 February 2014, the Swarm orbit was within the 0700 and 1900 local time sectors on the ascending and descending arcs, respectively. As time progresses, earlier local times are sampled. That means, we are entering northern summer conditions when

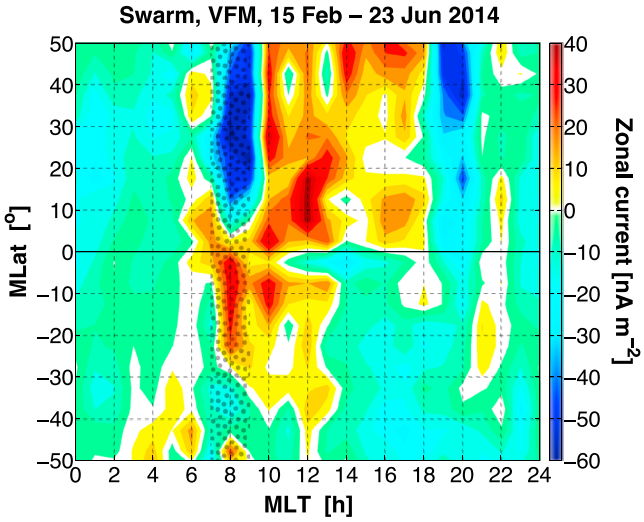

Figure 5. Magnetic local time (MLT) versus magnetic latitude (MLAT) distribution of mean zonal current at 490 km altitude. Positive values represent eastward currents. The current distribution around 08 MLT is regarded unreliable and therefore covered by a hashed bar.

sampling the local times before 1300 MLT. Thus, a part of the differences between prenoon and afternoon may be attributed to seasonal variation. On the nightside there is no indication of a seasonal variation.

5. Uncertainty of Zonal Current Density Estimates

The obtained average zonal *F* region currents are rather weak with respect to the resolution that can be obtained with our dual-satellite technique. For that reason it is important to consider the uncertainties associated with the processing approach. Here we follow the same line of arguments as used by *Ritter et al.* [2013] for estimating the uncertainties of radial currents. The same basic assumptions are as follows:

1. A bias, *bmf*, of any magnetic field component up to 1 nT, which is assumed to be constant for at least 5s, the time difference between measurements at the two quad points.
2. The resolution (digitization noise), *rmf*, of any field reading is amounting to 0.1 nT.
3. Each magnetic field reading has thus an uncertainty of $bmf \pm rmf$.
4. Position errors are negligible.

These numbers represent performance characteristics of the Swarm Level-1b magnetic field data products. Following the processing steps as outlined in *Ritter et al.* [2013] we reach at their final equation (24). Bias values of the vertical components cancel out since they are added with opposite signs. Only biases in the along-track component contribute.

$$\Delta j_y = \frac{1}{\mu_0}\left(\sqrt{bmf_{SW1}^2 + bmf_{SW2}^2} \pm \sqrt{2rmf_{SW1}^2 + 2rmf_{SW2}^2}\right)/dl_2 + \left(\sqrt{2rmf_{SW1}^2 + 2rmf_{SW2}^2}\right)/dl_1 \qquad (3)$$

where subscripts SW1 and SW2 stand in our case for Swarm A and Swarm B, respectively. When inserting the values for *bmf* (1 nT) and *rmf* (0.1 nT) and for dl_1 (along track: 38 km) and dl_2 (vertical separation: 48 km), we obtain a formal uncertainty of 30 nA/m^2. This is larger than most of the average current values. We may conclude that the systematic errors of our data are smaller than the Swarm Level-1b magnetic field performance characteristics. In any case, the zonal currents in the topside *F* region are weak and at the limit of the Swarm resolution.

On Figure 4 we see that current densities are highly variable in time and space. For quantifying the variability the standard deviation is calculated from the values within each bin used for Figure 5. However, for estimating the reliability of the mean values we have divided the standard deviations by the square root of the number of independent samples. Figure 6 shows the derived uncertainty of the mean current density presented in Figure 5. At night the values seem to be stable. At daytime, in particular, in the Northern (summer) hemisphere, the uncertainty significantly increases peaking at low latitudes around 0800 MLT.

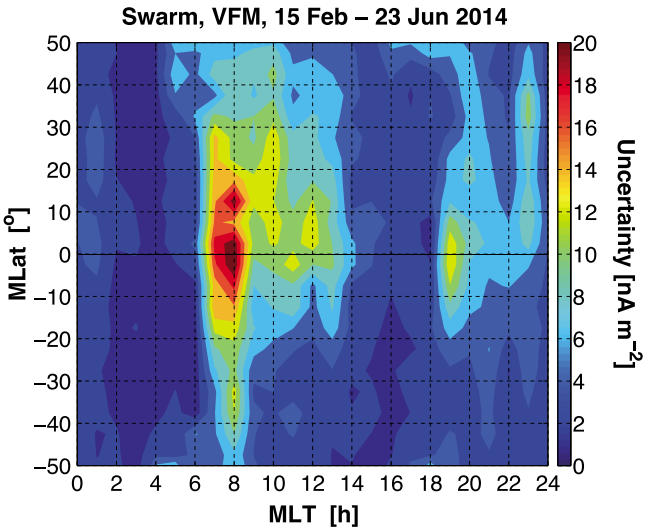

Figure 6. Uncertainty of the mean zonal current density as shown in Figure 5. For details see text.

For the discussion of the reliability it is important to take into account the increasing longitudinal (local time) separation between the Swarm A and B orbits. At the beginning of the study period, 15 February 2014, the orbits are only 0.5° apart in longitude. These reliable results are obtained at 1900 MLT (see Figure 4). Toward earlier local times the separation increases and with it the uncertainty. Finally, at 0800 MLT we have reached an orbit separation of 7.8° in longitude (or 32 min in local time). In that case the assumption of magnetic field measurements in a meridional plane is badly violated. Other currents in addition to zonal (e.g., field-aligned) make significant contributions to the magnetic field components considered in our analysis. For that reason we regard the dominant westward current in the Northern Hemisphere around 0800 MLT (covered by a hashed bar) as an artifact. Unfortunately, the Swarm mission does not provide more favorable orbit constellations for obtaining improved zonal current density estimates in this local time sector.

6. Discussion

We have analyzed the mean zonal current density in the altitude range 470 to 520 km at middle and low latitudes from magnetic field measurements of the Swarm constellation. In general, current densities are low, around 20 nA/m^2 on the dayside and 10 nA/m^2 on the nightside. In particular, the latter value is of interest for magnetic main field modelers who assume that there are no significant currents on the nightside at satellite altitude because the interpretation of magnetic field readings in terms of a scalar potential requires measurements in current-free space. The derived mean current density of 10 nA/m^2 seems to satisfy this requirement on the nightside rather well.

6.1. Comparison With Earlier Results

Quite comparable mean zonal current densities have been reported in earlier studies [e.g., *Shore et al.*, 2013; *Tozzi et al.*, 2015]. The study by *Shore et al.* [2013] was based on a combination of Ørsted and CHAMP data. Due to the rather different orbits of the two spacecraft, only short periods of close spatially overlapping data segments could be interpreted. The authors thus provided individual latitude profiles of horizontal current density. No attempt is made to retrieve the complete local time variation. The presented current densities scatter a lot both in amplitude and sign. This is consistent with our observations. Also, the average current density level is comparable with the values we retrieved. Their approach may have enlarged the scatter since they interpreted the magnetic field difference between the spacecraft second-by-second. This can result in spatial aliasing because small-scale features will influence only the readings of one of the two spacecraft separated by 300 to 400 km. We tried to avoid this problem by low-pass filtering the magnetic field readings before analysis. In addition, the smaller altitude difference of about 50 km between Swarm A and B minimizes aliasing effects.

Tozzi et al. [2015] used a different approach. For estimating the current density components in the layer between the upper and lower Swarm spacecraft they applied the curl-B approach to spatially binned magnetic field averages. The purpose of the study was mainly to check the influence of possibly existing horizontal currents in the topside ionosphere that could influence the main field magnetic field modeling. For that reason they limited their data selection to the nightside and to magnetically quiet times. Results are only presented for two local time sectors, one before midnight and another after midnight. Consistent with our results, they find predominantly westward currents in both hemispheres. Also, the current density ranging around 10 nA/m^2 agrees well with our nightside values. Unfortunately, the more interesting dayside currents have not been investigated.

6.2. Relevant Current Drivers

Here we want to discuss in more details the mechanisms that may be responsible for the observed currents. Equation (4) summarizes all the relevant contributions to the total current, **j**, in the ionosphere [e.g., *Kelley,* 2009]:

$$\mathbf{j} = \underline{\underline{\boldsymbol{\sigma}}}\,(\mathbf{E}+\mathbf{u}\times\mathbf{B}) + \{N_e\, m_i \mathbf{g}\times\mathbf{B} - k\nabla[(T_i + T_e)N_e]\times\mathbf{B}\}\frac{1}{B^2} \tag{4}$$

where $\boldsymbol{\sigma}$ is the conductivity tensor, **E** is the electric field, **u** the thermospheric wind velocity, N_e, is the electron density, m_i is the ion mass, **g** is the gravitational acceleration, k is the Boltzmann constant, T_e and T_i are the electron and ion temperature and **B** is the ambient magnetic field. Important drivers for the currents are, as listed in equation (4) from right to left, the plasma pressure gradient, the Earth's gravity, thermospheric winds, and finally electric fields, both imposed from outside and polarization fields caused by the divergence of current components.

The gravity-driven current is always flowing eastward. The direction of currents caused by the pressure gradient depends mainly on the ionospheric F_2 peak height. Above the peak currents flow westward and below eastward. For the zonal currents mainly meridional and upward winds are important. Quite important in that context is the diurnal wind variation, which is directed poleward and upward on the dayside, due to atmospheric expansion and equatorward on the nightside. This causes westward currents on the dayside and eastward on the nightside. Finally, there is a large-scale accumulation of positive charges on the dawnside and negative charges at dusk [*Kelley*, 2009]. This causes a zonal polarization E field, which drives eastward currents on the dayside and westward currents at night.

The various in situ observations of the Swarm satellites can be used to estimate the contributions from the different current drivers. The gravity-driven current is best constrained by the observations. All the quantities contributing to that current are measured or well known (see equation (4)). For daytime hours we obtain an eastward current density of about 10 nA/m^2 at low latitudes when considering an electron density of $1\cdot10^{12}$ m^{-3} (see Figure 7). Toward middle latitudes the intensity drops off rapidly because of reduced electron density and decreasing angles between **g** and **B**. After midnight current densities are down by at least a factor of 10.

The plasma pressure gradient is expected to be directed downward since the sampled volume is generally above the F_2 peak height (except in some cases at the equator, see Figure 7). When assuming the sum of electron and ion temperatures to be 3000 K at daytime [e.g., *Lühr et al.*, 2003] and inserting a typically observed density gradient of $0.15\cdot10^{12}$ m^{-3}/50 km (see Figure 7) we obtain according to equation (4) a westward current density of 5 nA/m^2. After midnight this value also reduces by about an order of magnitude due to lower density.

The average eastward electric field at daytime is known to be fairly small, about 0.5 mV/m [e.g., *Fejer et al.*, 2008]. During night electric fields generally point westward reaching amplitudes of about 1 mV/m. When inserting a typical low-latitude Pedersen conductivity for the F region at daytime of $1\cdot10^{-5}$ S/m [e.g., *Park and Lühr*, 2012], we obtain an eastward current of 5 nA/m^2. A significantly weaker westward current is driven by the E field at night.

Finally, we have the influence of the meridional wind. At low latitude the contribution from the diurnal variation is small because of the small angle between the wind direction and the B field. At middle latitudes we can assume according to the horizontal wind model 07 wind model about 50 m/s poleward winds and a vertical

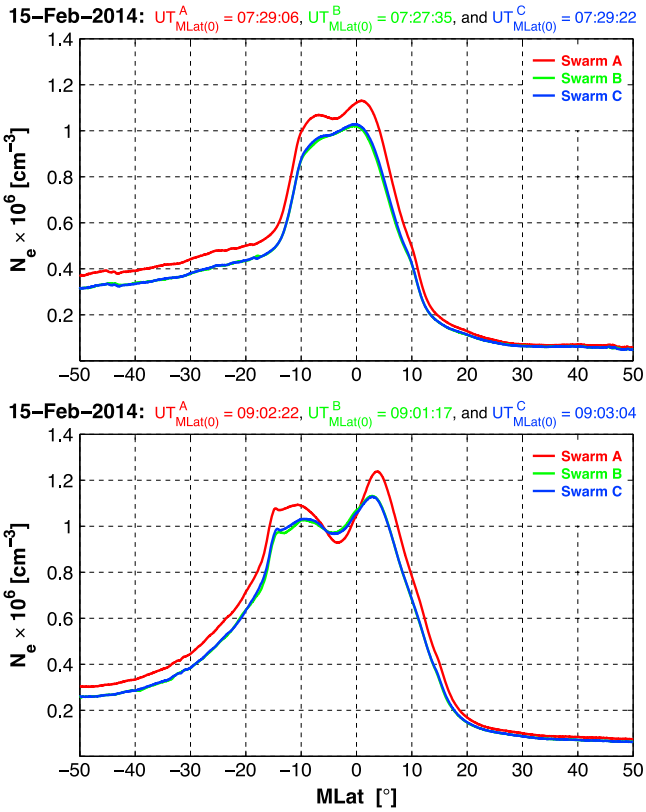

Figure 7. Electron density profiles from Swarm A, B and C corresponding to the current density profiles shown in Figure 4. Swarm A cruised at an altitude of 482 km and Swarm C at 506 km.

magnetic field component of 30–40 μT. In combination with the somewhat lower Pedersen conductivity at middle latitudes we can expect westward currents of about 3 nA/m^2 in both hemispheres during daytime. In this context we have to take into account that most of the daytime hours have been sampled at a season close to June solstice. During that time there is, in addition, an interhemispheric wind expected from summer to winter. This southbound meridional wind adds an eastward current component in the Northern Hemisphere and a westward current in the south.

When adding up all the listed components, we obtain a net current density that is in general agreement with the distribution in Figure 5. The stronger eastward currents in the Northern Hemisphere can be explained by the higher ion and neutral density in the summer hemisphere, and the slightly westward currents in the south are consistent with the contribution of the interhemispheric wind. The least constrained quantities, thermospheric wind and electric field, are probably responsible for the details of current distribution shown in Figure 5.

6.3. The Variability of Current Density

So far, we have discussed the mean value of the zonal currents. From the examples plotted in Figure 4 we know that the variability of horizontal currents both in time and space is significant. The standard deviation is on average 5 times larger than the uncertainty of the mean (Figure 6). Which means that the root-mean-square (RMS) value of the variations is typically twice as large as the mean value. In the quest for identifying the driver for this variability we may exclude the gravity-driven currents, which are determined by large-scale quantities. Also, the density-gradient currents are not a viable candidate, as can be deduced from the smooth *Ne* change shown in Figure 7, compared to the current variations in Figure 4. What remains are medium-scale electric field and wind variations. These are possibly caused by atmospheric gravity waves (GW) of comparable spatial scales. *Nakanishi et al.* [2014] and *Iyemori et al.* [2015] have reported about small-scale magnetic perturbations on the dayside, which are claimed to be caused by tropospheric phenomena. Largest perturbations are

observed during June solstice months, an interval well overlapping with our study period. *Park et al.* [2014, 2015] have shown the existence of thermospheric GW with horizontal wavelength of 150–600 km both on day and nightside. These GWs are believed to be driven from below because of their close spatial relation to GW activity centers in the stratosphere [e.g., *Jiang et al.*, 2003]. *Park et al.* [2014] report larger wave amplitudes in the winter hemisphere. This is in contrast with the observed variability of our horizontal currents (see Figure 6) where the northern summer hemisphere clearly dominates. More studies are needed for clarifying the mechanism responsible for the variability.

Resulting current fluctuations dissipate energy and thus should damp the waves. For Pedersen currents we can estimate the converted power, P, as

$$P = \frac{j_y^2}{\sigma_P}$$

Inserting a Pedersen conductivity of $1 \cdot 10^{-5}$ S/m and an observed RMS value for current variations of 40 nA/m^2, we obtain a power density of 0.16 nW/m^3. This is an appreciable wave damping and heating rate at 500 km altitude.

The apparent strong westward current in the Northern Hemisphere around 08 MLT is most probably an artifact. These data come from the end of the considered interval during June 2014. At that time the orbits of Swarm A and B are separated by 7.8° in longitude. Any vertical (field-aligned) current will falsely contribute to the zonal current estimate. In case of homogeneous current density the resulting magnetic field difference in along-track direction will scale with the separation of the tracks. Due to the longitudinal separation of about 800 km at that time, the effect of an upward vertical current of 5 nA/m^2 will be misinterpreted by equation (2) as a westward current of about 40 nA/m^2. This is the range of spurious current density shown in Figure 5 in the morning sector. From *Lühr et al.* [2015] we know that there are southbound interhemispheric field-aligned currents with densities of a few nA/m^2 at morning hours. We therefore have masked the time sector 07 to 09 MLT in Figure 5. Also, Figure 6 confirms the increasing uncertainties toward earlier local times and shows largest values around the 08 MLT sector. The disturbing influences of field-aligned currents increase linearly with the separation of the orbital planes.

7. Summary

We utilized magnetic field data from the early Swarm mission, when the longitudinal separation was quite small, for in situ zonal current estimates in the topside ionospheric *F* region. Simultaneous measurements at two altitudes are used to derive horizontal current densities. Suitable configurations for that are provided by the Swarm constellation only in the beginning after a separation in altitude (15 February 2014). The considered period lasted for about 130 days (23 June 2014), which is required for a full 24 h local time coverage. By the end of this period the assumption of measurements at two altitudes within the meridional plane was greatly compromised due to the increasing longitudinal separation of the orbital planes. In spite of that limitation, relevant characteristics of the zonal currents at 500 km altitude could be deduced.

1. Zonal currents are directed predominantly eastward on the dayside and westward at nighttime. The average current densities vary around 20 nA/m^2 and 10 nA/m^2 on day and nightside, respectively.
2. During daytime stronger currents are observed in the Northern Hemisphere. This may be attributed to the closer proximity of the study period to June solstice and thus larger electron density in the summer hemisphere. However, the given satellite sampling does not allow for a proper separation between seasonal and local time effects.
3. An assessment of relevant current drivers suggests that both eastward and westward contributions exist. During daytime the gravity-driven currents are expected to dominate the eastward currents at low latitudes. Interhemispheric winds from the Northern (summer) to Southern (winter) Hemisphere add an eastward current component in the north and a westward in the south.
4. Zonal currents show a high degree of variability both in time and space. The standard deviation of latitudinal profiles or from collocated measurements separated by only 2 min in time is more than double as large as the mean value. This is in particular true for the daytime summer hemisphere. We suggest that gravity waves originating from the lower atmosphere are responsible for the varying currents.

With the approach used here we could give a snapshot of zonal current characteristics. An extended study would allow a proper separate of seasonal from local time variations. Also, an investigation of longitudinal patterns would be desirable. With the given Swarm constellation other approaches for current estimation are needed to achieve that. A possibility may be statistics-based techniques for obtaining average characteristics of zonal current properties.

Acknowledgments
The authors are grateful to Jaeheung Park and Ingo Michaelis for fruitful scientific discussions during conducting this study. The European Space Agency (ESA) is acknowledged for providing the Swarm data and for financially supporting the work described in this paper. The data used here are principally based on Swarm Level-1b MAGx version 03xx data, freely accessible at https://earth.esa.int/web/guest/swarm/data-access. We have added a correction of the thermomagnetic effect. For details please contact the corresponding author.

References

Eccles, J. V. (2004), The effect of gravity and pressure in the electrodynamics of the low-latitude ionosphere, *J. Geophys. Res.*, *109*, A05304, doi:10.1029/2003JA010023.

Fejer, B. G., J. W. Jensen, S.-Y. Su (2008), Quiet-time equatorial *F* region vertical plasma drift model derived from ROCSAT-1 observations, *J. Geophys. Res.*, *113*, A05304, doi:10.1029/2007JA012801.

Finlay, C. C., N. Olsen, and L. Tøffner-Clausen (2015), DTU candidate field models for IGRF-12 and the CHAOS-5 geomagnetic field model, *Earth Planets Space*, *67*, doi:10.1186/s40623-015-0274-3.

Friis-Christensen, E., H. Lühr, D. Knudsen, and R. Haagmans (2008), Swarm—An Earth observation mission investigating geospace, *Adv. Space Res.*, *41*, 210–216, doi:10.1016/j.asr.2006.10.008.

Iyemori, T., K. Nakanishi, T. Aoyama, Y. Yokoyama, Y. Koyama, and H. Lühr (2015), Confirmation of existence of the small-scale field-aligned currents in middle and low latitudes and an estimate of time scale of their temporal variation, *Geophys. Res. Lett.*, *42*, 22–28, doi:10.1002/2014GL062555.

Jiang, J. H., D. L. Wu, S. D. Eckermann, and J. Ma (2003), Mountain waves in the middle atmosphere: Microwave limb sounder observations and analyses, *Adv. Space Res.*, *32*(5), 801–806, doi:10.1016/S0273-1177(03)00402-2.

Kelley, M. (2009), *The Earth's Ionosphere: Plasma Physics and Electrodynamics*, vol. 96, Academic Press (Elsevier), Boston, Mass.

Lühr, H., and S. Maus (2006), Direct observation of the *F* region dynamo currents and the spatial structure of the EEJ by CHAMP, *Geophys. Res. Lett.*, *33*, L24102, doi:10.1029/2006GL028374.

Lühr, H., M. Rother, S. Maus, W. Mai, and D. Cooke (2003), The diamagnetic effect of the equatorial Appleton anomaly: Its characteristics and impact on geomagnetic field modelling, *Geophys. Res. Lett.*, *30*(17), 1906, doi:10.1029/2003GL017407.

Lühr, H., G. Kervalishvili, I. Michaelis, J. Rauberg, P. Ritter, J. Park, J. M. G. Merayo, and P. Brauer (2015), The inter-hemispheric and *F*-region dynamo currents revisited with the Swarm constellation, *Geophys. Res. Lett.*, *42*, 3069–3075, doi:10.1002/2015GL063662.

Maus, S., and H. Lühr (2006), A gravity-driven electric current in the Earth's ionosphere identified in CHAMP satellite magnetic measurements, *Geophys. Res. Lett.*, *33*, L02812, doi:10.1029/2005GL024436.

Nakanishi, K., T. Iyemori, K. Taira, and H. Lühr (2014), Global and frequent appearance of small spatial scale field-aligned currents possibly driven by the lower atmospheric phenomena as observed by the CHAMP satellite in middle and low latitudes, *Earth Planets Space*, *66*, 40, doi:10.1186/1880-5981-66-40.

Olsen, N. (1997), Ionospheric *F* region currents at middle and low latitudes estimated from Magsat data, *J. Geophys. Res.*, *102*(A3), 4563–4576, doi:10.1029/96JA02949.

Park, J., and H. Lühr (2012), Effects of sudden stratospheric warming (SSW) on the lunitidal modulation of the *F*-region dynamo, *J. Geophys. Res.*, *117*, A09320, doi:10.1029/2012JA018035.

Park, J., H. Lühr, C. Lee, Y. H. Kim, G. Jee, and J.-H. Kim (2014), A climatology of medium-scale gravity wave activity in the midlatitude/low-latitude daytime upper thermosphere as observed by CHAMP, *J. Geophys. Res. Space Physics*, *119*, 2187–2196, doi:10.1002/2013JA019705.

Park, J., H. Lühr, M. Nishioka, and Y.-S. Kwak (2015), Plasma density undulations correlated with thermospheric gravity waves in the daytime low-latitude to midlatitude topside ionosphere, *J. Geophys. Res. Space Physics*, *120*, 6669–6678, doi:10.1002/2015JA021525.

Richmond, A. D. (1995), Ionospheric electrodynamics using magnetic apex coordinates, *J. Geomagn. Geoelectr.*, *47*, 191–212, doi:10.1029/92GL00401.

Rishbeth, H. (1971), The F-layer dynamo, *Planet. Space Sci.*, *19*, 263–267.

Ritter, P., H. Lühr, and J. Rauberg (2013), Determining field-aligned currents with the Swarm constellation mission, *Earth Planets Space*, *65*, 1285–1294, doi:10.5047/eps.2013.09.006.

Shore, R. M., K. A. Whaler, S. Macmillan, C. Beggan, N. Olsen, T. Spain, and A. Aruliah (2013), Ionospheric midlatitude electric current density inferred from multiple magnetic satellites, *J. Geophys. Res. Space Physics*, *118*, 5813–5829, doi:10.1002/jgra.50491.

Tozzi, R., M. Pezzopane, P. De Michelis, and M. Piersanti (2015), Applying a curl-B technique to Swarm vector data to estimate night-time *F*-region current densities, *Geophys. Res. Lett.*, *42*, 6162–6169, doi:10.1002/2015GL064841.